Swarm based Path-Following for Cooperative Unmanned Surface Vehicles

Marco Bibuli, Gabriele Bruzzone, Massimo Caccia, Andrea Gasparri, Attilio Priolo and Enrica Zereik.

***Abstract*—This paper proposes a swarm-based path-following guidance system for an autonomous marine multi-vehicle system. In particular, a team of Unmanned Surface Vehicles USVs is required to converge to and navigate along a desired reference path, while at the same time aggregating and maintaining a range-based formation configuration. Firstly, a separate description is given for a swarm methodology, initially developed for small ground mobile robots and exploited to aggregate the robot team, and a virtual target based path-following guidance system developed for USVs, exploited to drive not the single vehicles but the robot formation as a whole. Then, the integration of the two proposed methodologies is reported and proven, in order to guarantee the feasibility and stability of the overall guidance framework. Simulative results are proposed to validate the effectiveness of the proposed methodology and to evaluate the system performances.**

***Index Terms*—Path-Following, Swarm, Guidance, USVs**

I. Introduction

The goal of a continuous and widespread monitoring of large water areas, as well as intensive sampling and surveillance of oceans, harbors, lakes and rivers has brought in the recent years to the definition and the development of heterogeneous multi-vehicle frameworks, where a set of networked agents cooperates and coordinates themselves to achieve global objectives.

In particular, the need of fast-reliable, light-weight and low-cost vehicles is a key issue for the development of such multi-robot frameworks; the advantages with respect to huge and fully-equipped single-vehicle systems are obvious: multi-vehicle systems allow surveying of wider areas in less time, different sensing devices can be mounted on different vehicles thus lowering the cost of each single vehicle and achieving a higher robustness of the entire framework, avoiding to jeopardize the entire mission if a single robot or sensor fails or gets damaged. Moreover, the tasks of each agent can be re-planned to achieve different sampling resolution of the zones of interest. Being Unmanned Surface Vehicles (USVs) the interface between water and air environments, they are often also used as mobile communication relays between Autonomous Underwater Vehicles (AUVs) and remote control stations. For this reason, a number of studies and researches are dedicated to the coordination of such kind of vehicles. The main goal of the work presented in this paper is to merge a virtual target based path-following guidance module developed for marine surface vehicle systems, with a cooperative swarm methodology initially developed for small ground mobile robots. The work relies on the intuitive idea of developing a swarm aggregation behavior by means of a simple potential-based attraction/repulsion strategy, while using the path-following guidance system to guide the centroid of the robots' formation, and thus the swarm in a whole, onto a desired path.

The paper is organized as follows: section II reviews the state of the art of the swarm robotics literature, section III presents some theoretical preliminaries required to introduce the problem statement detailed in section IV. A review of the dynamics' modeling of unmanned surface vehicles and related control schemes is reported in section V. The swarm and path-following techniques are presented in section VI and VII respectively. The integration of the two approaches to achieve the goal of formation aggregation and guidance is reported in section VIII. Simulative results are reported and described in section IX, giving final conclusions in section X.

II. Related Work

A large literature regarding robot swarms has appeared in the last two decades. The paper [36] by Reynolds is one of the pioneering works on this subject. The author introduces a model for the motion of flocks of birds where the behavior of each individual is simulated independently. Three basic rules governing the interactions among the birds in the flock are identified:

- **Collision Avoidance**: the members have to avoid collisions among them and between them and environment.
- **Velocity Matching**: each member has to match the speed of its neighbors.
- **Flock Centering**: each member has to remain close to its neighbors.

In [35], the social potential field method is used to control a large scale multi-robot system. This method consists in designing the interaction functions governing the behavior of each individual w.r.t. its neighbors. Note that, these social potential fields agree with the rules proposed by Reynolds in [36]; in particular, the repulsive term matches with the collision avoidance rule, while the attractive term with the flock centering one. One of the first complete theoretical analysis concerning the stability of a swarming aggregation algorithms is given in [2], where a linear asynchronous model

M. Bibuli, G. Bruzzone, M. Caccia and E. Zereik are with the Istituto di Studi sui Sistemi Intelligenti per l'Automazione, Consiglio Nazionale delle Ricerche, 16149 Genova, Italy marco.bibuli@ge.issia.cnr.it

A. Priolo and A. Gasparri are with the Dipartimento di Ingegneria, Università degli Studi "Roma Tre", Via della Vasca Navale, 79 Roma 00146 Italy {gasparri, priolo}@dia.uniroma3.it

Authors are listed in alphabetical order.

This research received no specific grant from any funding agency in the public, commercial, or not-for-profit sectors.

is presented and its convergence properties are analyzed.
In the last decade, several swarming aggregation algorithms have been proposed [23], [22], [11], [30], [13], [31]. In [23], the authors introduce a decentralized continuous-time model for finite-time swarm aggregation. The analyzed interaction function if composed of a linear term to model the attraction and an exponential term for the repulsion. A bound on the radius of the convergence area is given along with the time required by the swarm to reach it. The results of this work are extended in [22] where classes of attractive and repulsive functions are considered. In particular, a theoretical analysis on the stability of the system and the ultimate boundedness of the trajectory of the swarm is given. In [11], the assumption of isotropic sensing among the robots is released generalizing the model in [23]. The circular area where the swarm converges into is detailed in terms of its radius and the stability of the swarm is proven. The well-known Vicsek model is extended in [30] by using an adaptive velocity swarm model. In [13], a swarm aggregation control law for unicycles is proposed. The control law is composed of a term for guaranteeing the collision avoidance and a second term to keep the robots in a compact configuration preserving the links among them. Eventually, a bound on the size of the region of convergence is detailed. In [31], a swarming algorithm for general sensing digraph with not unitary weights on the edges is presented. Indeed, the approach given in [22] is extended paving the way to a more generalized framework. Some works consider, also, the inevitable presence of actuator saturations. In [14], a set of control laws to drive the robots from any initial condition towards a desired configuration taking into account constraints on the inputs is provided. In [28], a behavior-based approach to formation maneuvers for groups of mobile robots that works under the assumption of constrained input is proposed. In [6], a flocking algorithm for a multi-agent system with bounded control inputs is proposed; the agents are able to achieve all the same velocity under the assumption of the connectivity of the underlying communication graph. A formation control scheme for multiple unicycles with saturated inputs is described in [27].

The motion coordination of USVs with the aim of providing and maintaining a communication infrastructure is of relevant importance, as exploited in the AOSN (Autonomous Ocean Sampling Network) Project, presented in [12] and [16], where an extended interconnection between underwater, surface and aerial vehicles is provided. For all of these reasons, a number of approaches and techniques have been developed in order to guide and control the motion of teams of marine vehicles. First at-field experiments were carried out to test and validate collision avoidance strategies for USVs based on COLREGS rules, like in [3]. On September 2008 in Trondheimsfjord (Norway), the first full-scale vehicle-following experiment in a civilian setting worldwide was carried out. The experiment involved a manned vehicle, a 30 m long research vessel with upper speed of 13 knots, followed by a retrofitted leisure boat of length 8.5 m with a maximum speed of 18 knots as USV [7]. The following year the experiment was replicated with a couple of slave vehicles following the master vessel [8]. A similar experiment was carried out by CNR-ISSIA with the Charlie USV following the dual-mode ALANIS vessel [5] Successful results have been also gained by the European Project GREX [1], [38] where one of the main project goals was the creation of a conceptual framework and middleware systems to coordinate a team of heterogeneous robotic vehicles, presenting interesting ideas about the control laws to be adopted in order to obtain an effective cooperative behavior.

The work in [15] possibly represents the best reference on the subject of exploitation of swarm approaches for the guidance of multi-vehicle marine robots. In this works, the authors propose a cooperative manipulation architecture for polygonal objects by a USV swarm. The main drawback of this work is that a full information sharing among the robots is required. The work in [18] shows a simulation about a team of autonomous vehicles that can be equipped with different sensors with the aim to gather data for ocean monitoring missions, e.g. about topics such as human-induced nutrification of coastal waters and the increasing industrial pollution; such issues require a reliable access to vast amounts of ocean-observation data. Some of the previous paper's authors presented another work (for details refer to [25]) about a distributed control algorithm for mobile aquatic sensor networks. Researches on marine robotic swarming, presented in [19] and [40], prove the great importance of the development of swarm control algorithms, in these cases applied to the oil pollution and to the the critical target localization and enemy engagement problems, respectively. Finally, issues about the security challenges for swarm robotics are described in [24] and [39].
The great interest for the marine robot swarms and the large number of possible applications, partially described in the literature, emphasize the importance to obtain actual algorithms for the team control and to develop a system of real vehicles able to effectively perform the established mission.

III. Preliminaries

From a mathematical point of view, as proposed in [22], [21], [20], the swarm system is composed by a set X of n robots, each one characterized by the vector $x_i(t) \in \mathbb{R}^m$ with $i = 1, \ldots, n$ of cartesian coordinates on the horizontal plane. Let us denote with $\bar{x}(t) = \frac{1}{n}\sum_{i=1}^{n} x_i(t)$ the (instantaneous) barycenter of the swarm and let us denote with $\epsilon_i(t) = x_i(t) - \bar{x}(t)$ the vector distance of each agent i from it. Furthermore, let us denote with $\chi(t) = \left[x_1(t) \ldots x_n(t)\right]^T$ and $\epsilon(t) = \left[\epsilon_1(t) \ldots \epsilon_n(t)\right]^T$, where $\chi(t), \epsilon(t) \in \mathbb{R}^{nm}$, the collection of all the agents locations and distances from the barycenter, respectively. To simplify the notation, in the rest of the paper the time dependency will be omitted when implied by the context.

The interactions among the robots can be described by an undirected proximity graph $\mathcal{G} = \{V, E\}$, where $V = \{v_i : i = 1, \ldots, n\}$ is the set of nodes (agents) and $E = \{\epsilon_{ij}\}$ is the set of edges (connectivity) representing the point-to-point communication channel available among the agents. An edge ϵ_{ij} exists if the agents i and j are within their visibility range R, that is: $\|x_i - x_j\| \leq R$. As the graph

is undirected the existence of the edge ϵ_{ij} (from node i to node j) implies the existence of the edge ϵ_{ji} (from node j to node i). Therefore, in the following they will be used without distinction to indicate a connection between agents i and j. Let us denote with $A(\mathcal{G})$ the adjacency matrix, that is a $n \times n$ matrix whose generic element $a_{ij} = 1$ if $i \neq j$ and $\epsilon_{ij} \in E$, $a_{ij} = 0$ otherwise. The number of the incoming edges $\Delta_i(\mathcal{G})$ of node i is called the *degree*. We define $\Delta(\mathcal{G})$ as the degree matrix: it is a $n \times n$ diagonal matrix whose elements are $\Delta_i(\mathcal{G})$, i.e., the degree of node i. In the following we will refer to $\mathcal{N}_i$ as the neighborhood of agent i, namely the set of indices of the agents directly connected through an edge with agent i. Clearly, it is $|\mathcal{N}_i| = \Delta_i(\mathcal{G})$. Finally we define the Laplacian matrix of a graph $\mathcal{G}$ as $\mathcal{L}(\mathcal{G}) = \Delta(\mathcal{G}) - A(\mathcal{G})$. To simplify the notation we will refer to it as $\mathcal{L}$ dropping its dependence on $\mathcal{G}$ unless strictly required.

Let us now review some properties of the Laplacian of an undirected graph. First of all, $\mathcal{L}$ is a weakly diagonal dominant symmetric matrix by construction. Furthermore we have that the row sum and the column sum are each equal to zero. In particular any graph Laplacian has always at least one null structural eigenvalue whose corresponding eigenvector is the vector of ones $\mathbf{1}$ of appropriate dimensions; in other words $\forall\, \mathcal{G},\ \mathcal{L}(\mathcal{G})\,\mathbf{1} = \mathbf{0}$ and $\mathbf{1}^T\mathcal{L}(\mathcal{G}) = \mathbf{0}^T$. The number of null eigenvalues corresponds to the number of connected components of $\mathcal{G}$ and $\texttt{Rank}(\mathcal{L}(\mathcal{G})) = n - c$ where n is the number of nodes and c is the number of connected components of $\mathcal{G}$; for details refer to [34]. All the eigenvalues of the Laplacian are real and positive in $[0, 2\,\Delta_{max}(\mathcal{G})]$, where $\Delta_{max}(\mathcal{G})$ is the maximum degree between the nodes in the graph, as it can be proved by applying the Gershgorin disc theorem as in [34]. Furthermore, the second smallest eigenvalue λ_2, namely the algebraic connectivity, provides an information regarding the connectedness of the graph.

IV. Problem Statement

The task of swarm aggregation is to define a proper interaction law to implement the three basic rules mentioned in section II, namely collision avoidance, velocity matching and flock centering. Furthermore, this control law should be based on local information and computed independently by each agent of the swarm leading to a complete decentralized and distributed aggregation approach. In order to achieve that, the following basic assumptions are required:

i) each robot knows its position with respect to a common reference frame - satisfied by reliability of GPS position measurements available onboard each USV, or alternatively by exploiting distributed algorithms as in [17];
ii) a reliable network infrastructure is needed to support inter-robot decentralized communication for position data sharing - WiFi systems can provide multi-access communication framework for data exchange.

Regarding the network infrastructure, it should be noticed that the connectivity maintenance is a relevant problem especially if the agents are moving in a cluttered environment. Nevertheless, this problem has been widely investigated in the robotics community (see [41], [37]) and thus it will not be object of this work.

While the swarm methodology fulfills the task of vehicle formation aggregation, the parallel task of driving such a formation onto a desired reference path has to be carried out. This latter goal is fulfilled by means of a virtual target based path-following approach developed in [4].

This task is carried out not directly driving the motion of each robot, but guiding the whole swarm. In particular the goal is to drive the instantaneous center of mass of the swarm towards the path, i.e., converging to a proper virtual target that moves along the path itself. To achieve such a goal, a proper velocity is computed and imposed to the swarm aggregation algorithm, which in turn will drive the motion of each vehicle according to such reference velocity. A schematic representation of the problem is reported in Fig. 1.

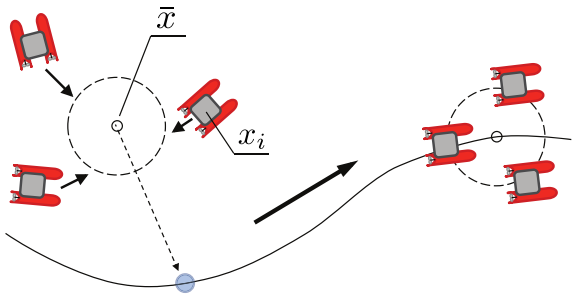

Fig. 1. Swarm aggregation and convergence to the path (on the left), swarm maintenance and path following (on the right).

V. Dynamics

For the dynamical representation of small size USVs, practical models are used for the aim of guidance and control system design. The term *practical* refers to the consistency, from the point of view of the accuracy degree, to the quality in terms of noise and sampling rate of the measurements provided by the sensors on-board the vehicles.

The models for the yaw-rate and surge velocity dynamics are represented by the following non-linear form, already described in [10] and [9]:

$$\tilde{m}_u \dot{u}_r = \tilde{k}_{u_r^2} u_r^2 + \tilde{k}_{\bar{n}^2\delta^2} \bar{n}^2 \delta^2 + \bar{n}^2 \quad (1)$$

$$\tilde{I}_r \dot{r} = \tilde{k}_{r|r|} r|r| + \tilde{k}_{\bar{n}^2} \bar{n}^2 + \bar{n}^2 \delta \quad (2)$$

where δ is the rudder angle, $\tilde{m}_u$ and $\tilde{I}_r$ are the inertia terms, $\tilde{k}_u$, $\tilde{k}_{u_r^2}$, $\tilde{k}_r$ and $\tilde{k}_{r|r|}$ are the drag coefficients, $\tilde{k}_{\bar{n}^2\delta^2}$ represents the resistance due to the rudder, and $\tilde{k}_{\bar{n}^2}$ takes into account the vessel longitudinal asymmetries, which change with the different payload configurations.

In order to design linear and angular velocity controllers, the dynamical models given by eq. (1) and eq. (2) have been considered, neglecting, i.e. considering as external disturbances, the resistance due to the rudder and the vessel longitudinal asymmetries. The result is the following generic 1-dof model for surge and yaw motion:

$$\tilde{m}_\xi \dot{\xi} = \tilde{k}_\xi \xi + \tilde{k}_{\xi|\xi|} \xi|\xi| + \tau \quad (3)$$

where $\tilde{m}_\xi$, $\tilde{k}_\xi$ and $\tilde{k}_{\xi|\xi|}$, τ represent inertia, linear and quadratic drag coefficients and control action respectively.

On this basis, a *PI* (Proportional Integral) gain scheduling controller can be adopted, considering eq. (3) as a generic nonlinear model:

$$\tilde{m}_\xi \dot{\xi} = f(\xi) + \tau \tag{4}$$

According to the work in [26], it is possible to design a parameterized family of *PI* linear controllers at each constant operating point ξ, obtaining a desired characteristic equation for the closed-loop linearized system in the form

$$s^2 + 2\sigma s + \sigma^2 + \omega_n^2 = 0 \quad , \quad \sigma > 0 \tag{5}$$

which does not depend on the particular constant operating point.

With this solution the velocity control for both surge and yaw-rate dynamics is achieved; anyway regarding the yaw control, sometimes it is more convenient to command the desired orientation, i.e. the vehicle direction of motion, rather than the velocity of rotation. To cope with this task, defining the actual direction of motion ψ as pointed out in [9] and the desired motion orientation ψ^*, a solution is proposed in [33], by means of the development of an Integral–Proportional–Derivative (I–PD) type, in which the control difference is fed to the controller output through the integral channel only. Therefore, abrupt changes in desired heading are not passed directly to the actuators, resulting in smooth actuation signals:

$$N = K_{I\psi} \int_0^t (\psi^* - \psi)\, dt - K_{P\psi}\psi - K_{D\psi}\dot{\psi} \tag{6}$$

Properly setting the three control parameters $K_{I\psi}$, $K_{P\psi}$ and $K_{D\psi}$ as described in [33], a third-order linear transfer function is obtained:

$$\frac{\psi}{\psi^*} = \frac{1}{a_{3\psi}s^3 + a_{2\psi}s^2 + a_{1\psi}s + 1} \tag{7}$$

VI. Swarming Algorithms for Multi-Robot Systems

In order to apply swarming algorithms originally developed for multi-robot systems to fleet of unmanned surface vehicles, let us review the approaches proposed in [22], [21], [20].

Let us consider a swarm composed of n robots with a network topology encoded by an undirected *fully connected* graph $\mathcal{G} = \{V, E\}$. As in [22], consider the following dynamics for each robot i:

$$\dot{x}_i = \sum_{j \neq i} g(x_i - x_j) \tag{8}$$

where $g(\cdot)$ is the interaction function representing the function of attraction and repulsion between neighboring robots. Let us denote with $g_a(\cdot) : \mathbb{R}^+ \to \mathbb{R}^+$ and $g_r(\cdot) : \mathbb{R}^+ \to \mathbb{R}^+$ the attractive and repulsive contributions, respectively. The interaction function $g(\cdot)$ can be defined as follows:

$$g(y) = -y\, [g_a(\|y\|) - g_r(\|y\|)] \,, \quad \forall\, y \in \mathbb{R}^m. \tag{9}$$

Note that the interaction function $g(\cdot)$ given in eq. (9) is odd, namely $g(y) = -g(-y)$. This is an important feature of the interaction function $g(\cdot)$ that leads to an aggregating behavior. Note also that the term $y\, g_a(\|y\|)$ represents the actual attraction, whereas the term $y\, g_r(\|y\|)$ represents the actual repulsion; moreover they both act on the line connecting the two interacting individuals, but in opposite directions.

Let us consider the following assumptions for the attractive and repulsive functions:

Assumption 1: There exist a *unique* distance δ corresponding to which we have $g_a(\delta) = g_r(\delta)$. Moreover, we have $g_a(\|y\|) \geq g_r(\|y\|)$ for $\|y\| \geq \delta$ and $g_r(\|y\|) > g_a(\|y\|)$ for $\|y\| < \delta$.

Assumption 2: There exist corresponding functions $J_a(\|y\|) : \mathbb{R}^+ \to \mathbb{R}^+$ and $J_r(\|y\|) : \mathbb{R}^+ \to \mathbb{R}^+$ such that $\nabla_y J_a(\|y\|) = y\, g_a(\|y\|)$ and $\nabla_y J_r(\|y\|) = y\, g_r(\|y\|)$.

Assumption 3: The attractive and the repulsive terms have to fulfill the following requirements:

$$\begin{aligned} g_a(\|y\|) &\geq \alpha \\ g_r(\|y\|) &\leq \frac{\beta}{\|y\|} \end{aligned} \tag{10}$$

with $\alpha, \beta \in \mathbb{R}^+$.

In [22] the following properties were proven:

- **P1** The barycenter $\bar{x}$ of the swarm is stationary over time;
- **P2** The swarm converges to a steady configuration;
- **P3** The swarm moves towards and remains within a bounded region;
- **P4** The swarm reaches the bounded region in finite time.

In particular, the following characterization of the bounded region was provided in [22]:

Theorem 1. *Consider a swarm of n mobile robots with dynamics in* (8) *for which Assumptions 1,2 and 3 hold. Then as time progresses all the members of the swarm will converge to the following bounded region:*

$$\mathcal{B}_r = \left\{ x \in \mathbb{R}^m : \|x - \bar{x}\| \leq \frac{\beta}{\alpha} \right\}. \tag{11}$$

In [21] the authors extended these results by considering the additional constraint of limited interaction among robots according to the network topology encoded by the (time-varying) graph $\mathcal{G}(t)$. As a result, the dynamics given in eq. (8) is modified as follows:

$$\dot{x}_i = \sum_{j \in \mathcal{N}_i(t)} g(x_i - x_j), \qquad i = 1, \ldots, n \tag{12}$$

where $\mathcal{N}_i(t)$ is the time-varying neighborhood of agent i. The authors proved that under the assumption of preserving the connectivity of the network topology the properties discussed above still hold. Furthermore, they proved the bounded region not only to be a function of the parameters of the attractive and repulsive functions but also of the algebraic connectivity λ_2 of the Laplacian matrix encoding the network topology.

In particular, the following result was given in [21]:

Theorem 2. *Let us consider a swarm of robots for which Assumptions 1, 2 and 3 hold. Let us assume that each robot*

has the dynamics given in eq. (12) *with the interaction function* $g(\cdot)$ *defined according to eq.* (9)*. If the graph* $\mathcal{G}$ *remains connected over time the swarm moves towards and remains within a bounded region defined as:*

$$\mathcal{B}_r = \left\{ x \in \mathbb{R}^m \,:\, \|x - \bar{x}\| \leq \frac{\beta\, \Delta_{\max}(\mathcal{G})\sqrt{n}}{\lambda_2(\mathcal{L})} \right\} \tag{13}$$

where $\Delta_{\max}$ *is the greatest among the robots degrees.*

Notably, this result was further improved in [20] by modeling the saturations of actuators in the robots dynamics. As a consequence, the dynamics given in eq. (12) was modified as follows:

$$\dot{x}_i = k\, \frac{\sum_{j\in\mathcal{N}_i(t)} g(x_i - x_j)}{1 + \left\| \sum_{j\in\mathcal{N}_i(t)} g(x_i - x_j) \right\|}, \tag{14}$$

where $k \geq 0$ is the saturated gain and the interaction function it still given by eq. (9), under Assumptions 1,2 and 3.

A direct consequence of the actuator saturation constraint is the loss of property **P1**, i.e., the swarm barycenter is no longer stationary. This is due to the fact that, while the mutual effects of interacting robots are always symmetric in the model given in eq. (8), this is not true under limited visibility as if a saturation occurs. Nevertheless, the authors showed that the model given in eq. (14) still exhibits properties **P2-P3** while, regarding the **P4**, they proved that the swarm gets arbitrarily close to the bounded region in finite time.

In particular, by introducing a further assumption on the Laplacian matrix built with respect to the normalizing factor $f(x_i) = \frac{1}{1+\left\|\sum_{j\in\mathcal{N}_i(t)} g(x_i - x_j)\right\|}$, it is possible to establish the following theorem.

Theorem 3. *Let us assume that each robot has the dynamics given in eq.* (14) *with the interaction function* $g(\cdot)$ *defined according to eq.* (9) *under Assumptions 1,2, and 3. If the graph* $\mathcal{G}$ *remains connected over time the swarm moves towards and remains within a bounded region defined as:*

$$\mathcal{B}_r = \left\{ x \in \mathbb{R}^m \,:\, \|x - \bar{x}\| \leq \frac{\beta}{\alpha}\, \frac{(n-1)}{\lambda_{2,\min}} \right\}. \tag{15}$$

with $\lambda_{2,\min}$ *a lower bound on the Laplacian matrix algebraic connectivity.*

Proof. First of all, note that the existence of $\lambda_{2,\min}$ can be guaranteed by adapting the approach given in [37]. Then, consider the following Lyapunov candidate:

$$V(t) = \frac{1}{2} \sum_{i=1}^{n} \epsilon_i(t)^T\, \epsilon_i(t). \tag{16}$$

Its time derivative is (the bounds of the summation are omitted for compactness):

$$\dot{V}(t) = \sum_i \epsilon_i^T \dot{\epsilon}_i = \sum_i \epsilon_i^T (\dot{x}_i - \dot{\bar{x}}) = \underbrace{\sum_i \epsilon_i^T \dot{x}_i}_{\dot{V}_1} - \underbrace{\sum_i \epsilon_i^T \dot{\bar{x}}}_{\dot{V}_2}.$$

As reported in [20], the motion of the barycenter does not affect the size of the region where the swarm is going to aggregate, i.e., $\dot{V}_2 = 0$.

We now investigate the term $\dot{V}_1$. Without loss of generality, let us omit the constant k in (14). We have

$$\begin{aligned} \dot{V}_1 &= \sum_i \epsilon_i^T \frac{\sum_{j\in\mathcal{N}_i(t)} -g(x_i - x_j)}{1 + \| \sum_{j\in\mathcal{N}_i(t)} -g(x_i - x_j)\|} \\ &= \sum_i \epsilon_i^T \frac{\sum_{j\in\mathcal{N}_i(t)} -g(\epsilon_i - \epsilon_j)}{1 + \| \sum_{j\in\mathcal{N}_i(t)} -g(\epsilon_i - \epsilon_j)\|} \\ &= -\sum_i f(x_i) \epsilon_i^T \sum_{j\in\mathcal{N}_i(t)} g(\epsilon_i - \epsilon_j). \end{aligned} \tag{17}$$

Therefore, eq. (17) can be rewritten as follows:

$$\begin{aligned} \dot{V}_1 &= -\sum_i f(x_i) \epsilon_i^T \sum_{j\in\mathcal{N}_i(t)} g(\epsilon_i - \epsilon_j) \\ &= \underbrace{-\sum_i f(x_i) \left(\epsilon_i^T \sum_{j\in\mathcal{N}_i(t)} (\epsilon_i - \epsilon_j) g_a(\|\epsilon_i - \epsilon_j\|) \right.}_{\dot{V}_a} \\ &\quad \underbrace{\left. + \epsilon_i^T \sum_{j\in\mathcal{N}_i(t)} (\epsilon_i - \epsilon_j) g_r(\|\epsilon_i - \epsilon_j\|) \right)}_{\dot{V}_r} \end{aligned}$$

We now further investigate the term $\dot{V}_a$. Using the properties of the Laplacian matrix and Assumption 3, we have:

$$\begin{aligned} \dot{V}_a &= -\sum_i f(x_i) \epsilon_i^T \sum_{j\in\mathcal{N}_i(t)} (\epsilon_i - \epsilon_j)\, \alpha = -\alpha \epsilon^T \bar{\mathcal{L}}\, \epsilon \\ &\leq -\alpha \lambda_{2,\min} \sum_i \|\epsilon_i\|^2. \end{aligned} \tag{18}$$

where $\bar{\mathcal{L}} = \Gamma\, \mathcal{L}$, with Γ a diagonal matrix whose elements on the main diagonal are defined as $\gamma_{ii} = f(x_i)$. As far as $\dot{V}_r$ is concerned, the following holds:

$$\begin{aligned} \dot{V}_r &\leq \sum_i \epsilon_i^T \sum_{j\in\mathcal{N}_i(t)} (\epsilon_i - \epsilon_j)\, f(x_i)\, \frac{\beta}{\|\epsilon_i - \epsilon_j\|} \\ &\leq \sum_i \|\epsilon_i\| \sum_{j\in\mathcal{N}_i(t)} \|\epsilon_i - \epsilon_j\|\, f(x_i)\, \frac{\beta}{\|\epsilon_i - \epsilon_j\|} \\ &\leq \sum_i \|\epsilon_i\|\, \beta\, (n-1) \end{aligned} \tag{19}$$

Now combine eqs. (18) and (19) to get:

$$\begin{aligned} \dot{V}_1 &= \dot{V}_a + \dot{V}_r \leq -\alpha \lambda_{2,\min} \sum_i \|\epsilon_i\|^2 + \beta\, (n-1) \sum_i \|\epsilon_i\| \\ &\leq \sum_i \|\epsilon_i\| \Big(-\alpha \lambda_{2,\min} \|\epsilon_i\| + \beta\, (n-1) \Big) \end{aligned} \tag{20}$$

which is negative definite if

$$\|\epsilon_i\| > \frac{\beta}{\alpha}\, \frac{(n-1)}{\lambda_{2,\min}}. \tag{21}$$

Therefore, the solution of the system is bounded within the region:

$$\|x - \bar{x}\| \leq \frac{\beta}{\alpha}\, \frac{(n-1)}{\lambda_{2,\min}} \tag{22}$$

□

Note that differently from the analysis carried out in [20], in the proof of Theorem 3 the contribution given by the single ϵ_i to the time derivative of the Lyapunov candidate is considered. Indeed, this allow to obtain a more refined characterization of the swarm convergence area which does not involve the use of the max function. Furthermore, it should be noticed that the control law given in eq. (14) does not formally guarantee the collision avoidance among the swarm members. Nevertheless, this problem could be easily overcome by substituting (14) with the enhanced control law provided in [29]. Its integration will be subject of upcoming works.

VII. Path-Following Algorithm

The aim of this work is to develop a guidance system capable of driving the entire robotic formation, aggregated by means of the swarm behavior, towards and along a predefined reference path. A brief introduction to the essential concepts of the virtual target based path-following approach for single-vehicle guidance is given in this section (further details, proofs and experimental results can be found in [4] and references therein). Subsequently, such path-following approach is applied to the task of swarm path-following, not guiding the motion of each vehicle but providing the convergence to and the following of the path by the swarm in a whole.

By referring to Fig. 2 and assuming the vehicle's motion restricted to the horizontal plane, the task consists in the zeroing of both the position error vector $\underline{d}$, i.e. the distance between the vehicle and the virtual target attached to the *Serret-Frenet* frame $< f >$, and the orientation error $\beta = \psi - \psi_f$, where ψ and ψ_f are the vehicle's direction of motion and local path tangent respectively, expressed with respect to the earth-fixed reference frame $< w >$. Following the geometrical and

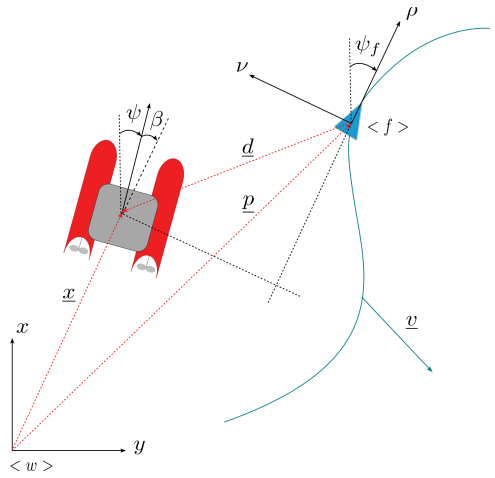

Fig. 2. Path-Following modeling framework.

kinematic analysis carried out in [4], the distance error model, expressed with respect to the frame $< f >$, has the following form:

$$\begin{cases} \dot{\rho} = (c_c\,\nu - 1)\,\dot{s} + U\cos\beta \\ \dot{\nu} = -c_c\,\dot{s}\,\rho + U\sin\beta \end{cases} \tag{23}$$

where c_c is the local path curvature, $\dot{s}$ is the speed of the virtual target along the path and U the total speed of vehicle (speed along the direction of motion) with respect to the earth-fixed reference frame. In order to solve the path-following problem for a single-vehicle system, the aim is to develop a proper approach angle function ψ^*, designed to reduce the linear error components (ρ and ν) to zero. Following the development carried out in [4], the desired angle ψ^* is a function of the cross-track error ν summed with the local path tangent, thus $\psi^* = \psi_f + \varphi(\nu)$, where the function $\varphi(\nu)$ is required to satisfy the following constraints:

$$|\varphi(\nu)| < \frac{\pi}{2} \quad ; \quad \nu\varphi(\nu) \leq 0 \quad ; \quad \varphi(0) = 0$$

Relying on a low level controller, providing an auto-heading regulator capable of tracking desired orientation profiles, it can be stated that considering $V_\psi = \frac{1}{2}(\psi - \psi^*)^2$ as the candidate Lyapunov function, the low level controller provides a behavior such that $\dot{V}_\psi \leq 0$, i.e. the vehicle orientation converges to the desired angle $\psi \to \psi^*$ and it can be rewritten as $\beta \to \varphi(\nu)$. Moreover it's worth noticing that when $\dot{V}_\psi = 0$, an invariant set is defined, in which the condition $\beta = \varphi(\nu)$ holds. The task of the path-following controller design is achieved by the definition of the Lyapunov function $V = \frac{1}{2}(\rho^2 + \nu^2)$; computing the time derivative of the function V, the following expression is obtained:

$$\begin{aligned} \dot{V} &= \rho\dot{\rho} + \nu\dot{\nu} \\ &= -\rho\dot{s} + \rho U\cos\beta + -\nu U\sin\beta \\ &= \dot{V}_\rho + \dot{V}_\nu \end{aligned}$$

substituting $\dot{\rho}$ and $\dot{\nu}$ with the equation system (23) and defining $\dot{V}_\rho = -\rho\dot{s} + \rho U\cos\varphi(\nu)$ and $\dot{V}_\nu = -\nu U\sin\beta$.
Following the methodology of [4], the speed of the reference frame $\dot{s}$, i.e. the velocity of the virtual target moving along the path, can be used as an additional control variable. Imposing

$$\dot{s}^* = K_\rho\rho + U\cos\beta \tag{24}$$

as the desired virtual target speed, where K_ρ is a tunable controller parameter, the function $\dot{V}_\rho$ assumes the following form:

$$\dot{V}_\rho = -K_\rho\rho^2 \leq 0 \tag{25}$$

About $\dot{V}_\nu$, recalling the above-mentioned assumption on the attraction to the invariant set defined by $\dot{V}_\psi = 0$, β can be substituted by $\varphi(\nu)$, obtaining:

$$\dot{V}_\nu = \nu U\sin\beta = \nu U\sin\varphi(\nu) \tag{26}$$

Selecting the function $\varphi(\nu)$ as

$$\varphi(\nu) = -\psi_a\tanh(K_\nu\nu) \tag{27}$$

with K_ν as a tunable controller parameter and $\psi_a \in \left[0; \frac{\pi}{2}\right]$ the maximum approach angle with respect to the local tangent ψ_f, the term $\nu U\sin\varphi(\nu)$ is ≤ 0 because of the assumption made on the function $\varphi(\nu)$.
Being both the terms $\dot{V}_\rho$ and $\dot{V}_\nu \leq 0$, thus entailing $\dot{V} \leq 0$, the global asymptotic stability for the path-following guidance system is proven.

VIII. Swarm based Path-Following

In this section, the proposed swarm based path-following algorithm for a fleet of unmanned surface vehicles is described. The idea is to provide a unified framework obtained by merging the path-following strategy originally developed in [4] for a single surface vehicle, with the swarming algorithm proposed in [20] and originally developed for teams of mobile robots. In particular, the following control input should be used for each USV:

$$\dot{x}_i = u_i^s + u^g \tag{28}$$

where the term u_i^s, different for each USV, is the control effort required to reach a collective behavior while the term u^g, common to all the USV, refers to the expected trajectory of the fleet centroid, computed with reference to section VII as:

$$u^g = \begin{bmatrix} u^* \cos\psi^* \\ u^* \sin\psi^* \end{bmatrix} \tag{29}$$

where u^* is the desired speed for the formation along the path and ψ^* is the reference guidance angle computed by the path-following module, i.e. the direction of motion that the overall swarm formation has to assume in order to converge to and follow the reference path.

An important issue that has often to be taken into account when developing techniques and algorithms for unmanned surface vehicles is the constraint of the one-directional surge motion: being many vehicles stern-propelled, they provide a backward motion (negative surge speed) which is many times less efficient with respect to the forward motion (positive surge speed). For this reason, marine vehicles are commanded to work only with forward motion, thus the positivity constraint of the reference speed has to be imposed. In the case of the proposed application of swarm path-following, the resulting reference velocity vector has to be generated maintaining the same π-sector direction of the path-following velocity contribution, i.e. $\angle(\dot{x}_i) \in [\angle(u^g) - \pi/2; \angle(u^g) + \pi/2]$. Thus the condition $\|u_i^s\| \leq \|u^g\|, \forall i$ has to be guaranteed in order to avoid: *i*) motion inversions, given by the sign change of the resulting reference $\dot{x}_i$; *ii*) steering behaviors generated by the $\dot{x}_i$ direction's change. From eq. (14), it can be stated that the swarm velocity contribution for the aggregation behavior is bounded by the value k, having $\|u_i^s\| \leq k, \forall i$. Thus, posing $k < \|u^g\|$, where $\|u^g\|$ represents the desired speed along the path, the fulfillment of the condition $\|u_i^s\| \leq \|u^g\|, \forall i$ is always guaranteed.

Finally, it should be noticed that in the case of a time variant desired path-following speed profile $u_g^* = u^*(t)$, the parameter k can be tuned over time to satisfy the positive surge speed constraint This can be achieved by simply choosing $k = \tilde{k}\, u^*(t)$ with $0 < \tilde{k} < 1$. Indeed, this would enforce the constraint:

$$\|u_i^s(t)\| < \|u^g(t)\| \quad \forall\, t \geq 0. \tag{30}$$

To the aim of investigating how the stability property of the two control terms is affected by their interaction, the analysis is carried out assuming the swarm to be moving in an obstacle-free environment. Regarding the swarming behavior, it should be noticed that since the guidance control term $u^g(t)$ is common to all USVs, the same stability analysis proposed in [20] can be considered by exploiting an opportune coordinate transformation to a frame which moves according to the guidance control term itself. Regarding the path-following algorithm, it should be noticed that the actual control term for each USV given in eq. (28) must fulfill the constraint given in eq. (30). This allows to compute an upper bound on the maximal instantaneous discrepancy $\Delta\psi$ between the desired motion direction ψ for the swarm centroid and the actual angle of the vector tangent to the centroid trajectory. More specifically, this can be obtained by considering the maximal discrepancy between the desired reference angle $\psi^\star$ and the angle of the velocity vector in eq. (28) for any USV, by assuming the two control terms to be orthogonal vectors, that is:

$$\Delta\psi = \max_{i \in 1,\ldots,N} \left\{ \arctan\left(\frac{\|u_i^s(t)\|}{\|u^g(t)\|} \right) \right\} \tag{31}$$

Furthermore, it should be noticed that according to the analysis carried out in [20] the aggregation control term $u_i^s(t)$ goes to zero as time goes to infinity, therefore the discrepancy $\Delta\psi$ is a vanishing term. Nevertheless, in order to investigate how this discrepancy affects the guidance of the swarm centroid during the transient phase of the swarm aggregation, eq. (26) is recalled and rewritten keeping into account the discrepancy term, thus obtaining:

$$\dot{V}_\nu = \nu U \sin(\psi^* + \Delta\psi - \psi_f) = \nu U \sin(\varphi(\nu) + \Delta\psi) \tag{32}$$

Applying trigonometric rules, the term $\sin(\varphi(\nu) + \Delta\psi)$ can be rewritten as

$$\frac{1}{\sqrt{\|u^g(t)\|^2 + \|u_i^s(t)\|^2}} \left[\|u^g(t)\| \sin\varphi(\nu) + \|u_i^s(t)\| \cos\varphi(\nu) \right]$$

where $\|u^g(t)\| \equiv U$, substituting this latter in eq. (32), the following form is obtained:

$$\dot{V}_\nu = \frac{\nu U}{\sqrt{U^2 + \|u_i^s(t)\|^2}} \left[U \sin\varphi(\nu) + \|u_i^s(t)\| \cos\varphi(\nu) \right]$$

Being the term $\|u_i^s(t)\|$ positive and bounded and $|\varphi(\cdot)| < \frac{\pi}{2}$ by definition, defining the term $\tilde{U} \doteq \sqrt{U^2 + \|u_i^s(t)\|^2}$, the $\dot{V}_\nu$ can be rewritten considering a positive disturbance term ϵ for the path-following module

$$\dot{V}_\nu = \frac{U}{\tilde{U}} \nu \left[U \sin\varphi(\nu) + \epsilon \right]$$

To achieve the stability requirement $\dot{V}_\nu \leq 0$, the following condition must hold:

$$U \sin\varphi(\nu) + \epsilon \leq 0$$

The analysis leads to the result that the path-following error component ν will be bounded by the limit value

$$\tilde{\nu} = \varphi^{-1}\left(\sin^{-1}\left(\frac{\epsilon}{U} \right) \right)$$

that is bounded for $\frac{\epsilon}{U} < \sin(1)$, limit that could be easily satisfied setting the gain k accordingly. It has to be recalled that ϵ is a vanishing term that tends to zero as the swarm aggregation is reached, thus the worst case analysis carried

out imposes limit conditions only during the transient phase of the swarm formation.

Some further remarks have to be reported concerning the issues of path curvature and number/position of vehicles in the swarm. It is obvious that during path-following execution, each vehicle is subject to a different curvature depending on its position with respect to the swarm centroid; vehicles on the border positions of the swarm and closer to the path curve center are subject to a greater curvature, as depicted in Figure 3. If such a curvature value cannot be assumed by the vehicle, the swarm will tend to disaggregate until the crucial part of the path has been passed. Being not possible to overcome the physical constraints imposed by the vehicles themselves, the problem has to be faced at planning level, i.e. designing the desired reference paths in such a way that the swarm formation could perform. To this aim, studies and researches can be found in literature regarding the issue of curvature constrained path planning, as for instance the work [32].

An estimation of curvature constraint can be anyway calcu-

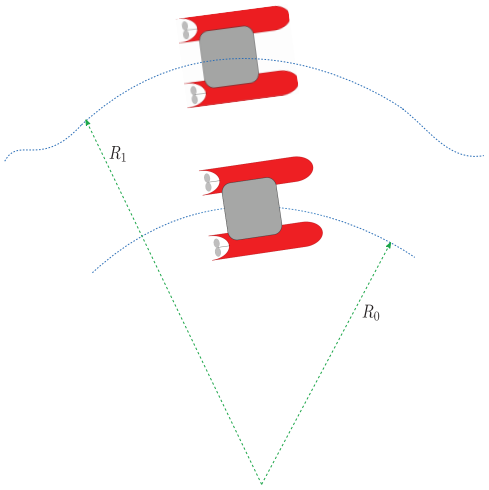

Fig. 3. Curvature assumed by robots during curve's motion.

lated making some simple assumptions. Considering a swarm of n vehicles, in order to evaluate the maximum curvature that the farther vehicles, with respect to the swarm centroid, will assume during curves, the worst a regime swarm configuration that has to be considered is the one where the vehicles assume a circular aggregation, as represented in Figure 4.

Being η the equilibrium distance of attraction/repulsion aggregation forces and $\alpha = \frac{2\pi}{n}$, the swarm radius can be computed by:

$$L = \frac{\eta}{\sin\frac{\alpha}{2}} = \frac{\eta}{\sin\frac{\pi}{n}}$$

Defining c_{c_p} the maximum curvature of the reference path and thus $R_p = 1/c_{c_p}$ the least curvature radius of the path, the most internal vehicles of the swarm will be subject to a curvature radius $R_i = R_p - L$, whose curvature value is $c_{c_i} = 1/R_i$, which in turn brings to the relations between curvatures $c_{c_p} = \frac{c_{c_i}}{1+Lc_{c_i}}$.
Considering $c_{c_{max}}$ the maximum curvature value that a vehicle can assume, thus the maximum curvature along the path must

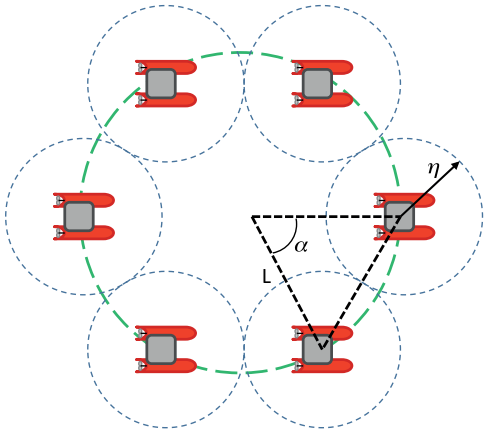

Fig. 4. Worst swarm configuration to evaluate maximum curvature assumed by the vehicles.

satisfy the condition

$$c_{c_p} \leq \frac{c_{c_{max}}}{1 + Lc_{c_{max}}}$$

in order to guarantee that the swarm will properly follow the reference path. Thus the c_{c_p} can be used as a constraint to generate suitable desired path references.

IX. Simulative Results

Being a set of small USVs (dimensions $<$ 1 m) actually under development, this section reports only simulative results, based on practical dynamical and kinematic models that fit with characteristics of the Charlie USV, as already introduced in section V and proven by the authors in [4], [10] and [9].

The closed loop dynamics' control has been implemented, for the sake of simplicity at simulation level, as stable linear transfer functions (for both the surge and yaw dynamics) as described in [9] and [33].
The results reported in this section are relative to a scenario where four vehicles are required to assume the desired formation, which is determined by the two attractive and repulsive potential functions respectively, derived from eq. (10):

$$\begin{aligned} g_a(d) &= \alpha \\ g_r(d) &= \frac{\beta}{(d - 2\eta)} \end{aligned} \tag{33}$$

where d is the Euclidean distance between two robots $\|x_i - x_j\|$ and η a safety region slightly larger than the physical space occupation of the vehicle. Note that, the term η, originally introduced in [22] for modeling agents with finite size, is meant to limit the interaction between the robots up to the distance 2η. Indeed, this allows to easily integrate a practical solution for the collision avoidance which as stated in the previous section of the paper cannot be guaranteed formally. In particular, an additional unbounded repulsive term g_{ca} can be enabled when two vehicles come close to a collision situation, i.e. when the relative distance assumes a value below 2η. From a mathematical point of view, equation (9) is modified in

$g(d) = -d\,[g_a(d) - g_r(d) - g_{ca}(d)]$ and the additional term g_{ca} has the form of:

$$g_{ca}(d) = \frac{2\eta - d}{d^2} \tag{34}$$

which is enabled when the condition $0 \leq d \leq 2\eta$ holds.
For all the experiments, the value of the attraction and repulsion function parameters are set to $\alpha = 1.0$, $\beta = 2.0$, $\eta = 3.0$.

The first reported experiment is focused on the analysis of the vehicles' motion during the pure swarm aggregation, thus setting the formation reference velocity u^g, with respect to eq. (28), as a constant vector with magnitude $|u^g| = 1$ m/s as desired cruise speed and a fixed course defined by $\angle(u^g) = \pi/2$. The trial is initialized with stationary robots, positioned in random locations; as soon as the trial is executed the vehicles' motions evolve driven by the swarm aggregation function, leading the robots to a regime position in the formation, as reported in Figure 5 where the solid lines represent the motion of the related vehicle and the dotted line is the motion of the formation centroid. The vehicles' motion is directed towards a $\pi/2$ course and the speed profiles of all the vehicles reach the cruise speed value of 1 m/s, as defined by the vector u^g, with reference to Figure 6. Regarding the velocity profiles, two main issues have to be discussed:

- the required velocity of each robot presents oscillations, due to the swarm aggregation functions; the characteristics of such an oscillatory behavior can be reshaped/attenuated by the definition of different attraction/repulsion functions. It has to be underlined that, for the particular case, such oscillations are in the bandwidth of the dynamics' controllers, thus the velocity reference can be tracked by the vehicle (this is reported in details in the further experimental results);
- the overall guidance system has to keep into account the physical limits of the vehicle that, for the particular case of the Charlie vehicle (and in general for small USVs), are given by the minimum (in term of the lowest speed at which the vehicle is capable of properly maneuver) and maximum (highest operative condition) surge speeds of about 0.5 and 1.5 m/s respectively. This issue is easily managed recalling the assumptions defined in section VIII: the speed contributions generated by the swarm aggregation function are bounded and belong to $(-k; k)$. Setting the value $k = 0.5$, then it can be guaranteed that the resulting surge speeds to be tracked are bounded by the limit values $|u^g| \pm k$, thus obtaining $u_{min} = 0.5$ and $u_{max} = 1.5$.

The second experiment combines the swarm aggregation behavior with the path-following guidance of the overall robots' formation, guiding the team to converge to and track a quasi-sinusoidal shaped path, defined by a 6^{th} order polynomial parametric curve.
The path-following module parameters have been set to:
$K_\rho = 1.0$, $K_\nu = 0.3$, $\psi_a = \pi/3$
The initial configuration is the same of the previous experiment, with a randomly generated initial position of the robots. Figure 7 shows the aggregation behavior combined with the motion towards the reference path. It can be noticed how the relative position of each vehicle within the formation is not fixed, but only constrained by the inter-vehicle distances; thus the position in the formation is only function of the initial position and evolution along the desired reference. Furthermore, it can be noticed how the formation centroid converges to and track the path for all the experiment, proving the validity of the approach. In Figure 8, for each vehicle, the actual surge speed and heading angle (blue lines) are compared with the generated speed and orientation references (red lines); u_1 and ψ_1 correspond to the blue vehicle, u_2 and ψ_2 correspond to the red vehicle, u_3 and ψ_3 correspond to the green vehicle, u_4 and ψ_4 correspond to the magenta vehicle. As introduced before, the surge speed and orientation tracking by means of the dynamics' controllers is achieved although the presence of the oscillations in the reference signals (only a tracking delay is introduced during the oscillatory regime).

A third experiment is focused on the overall behavior analysis in presence of disturbances affecting the vehicles'

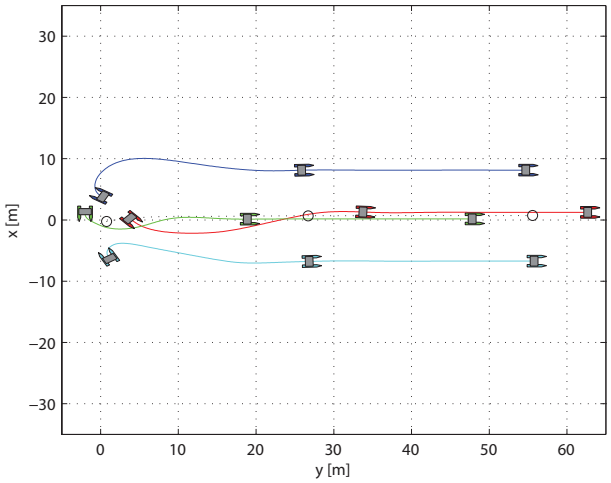

Fig. 5. Robots' motions during swarm aggregation evolution.

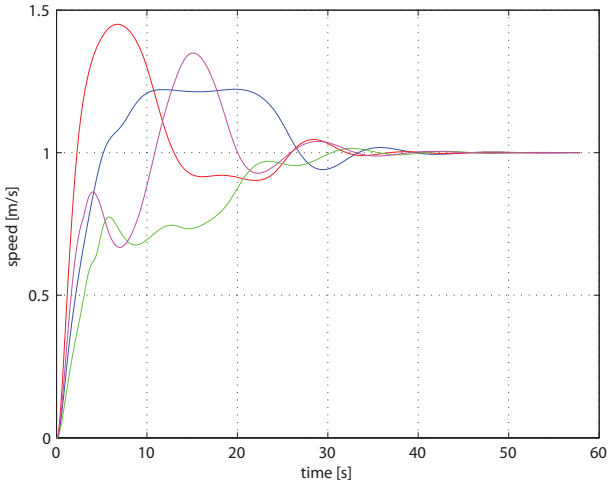

Fig. 6. Robots' speed profiles assumed during swarm aggregation evolution.

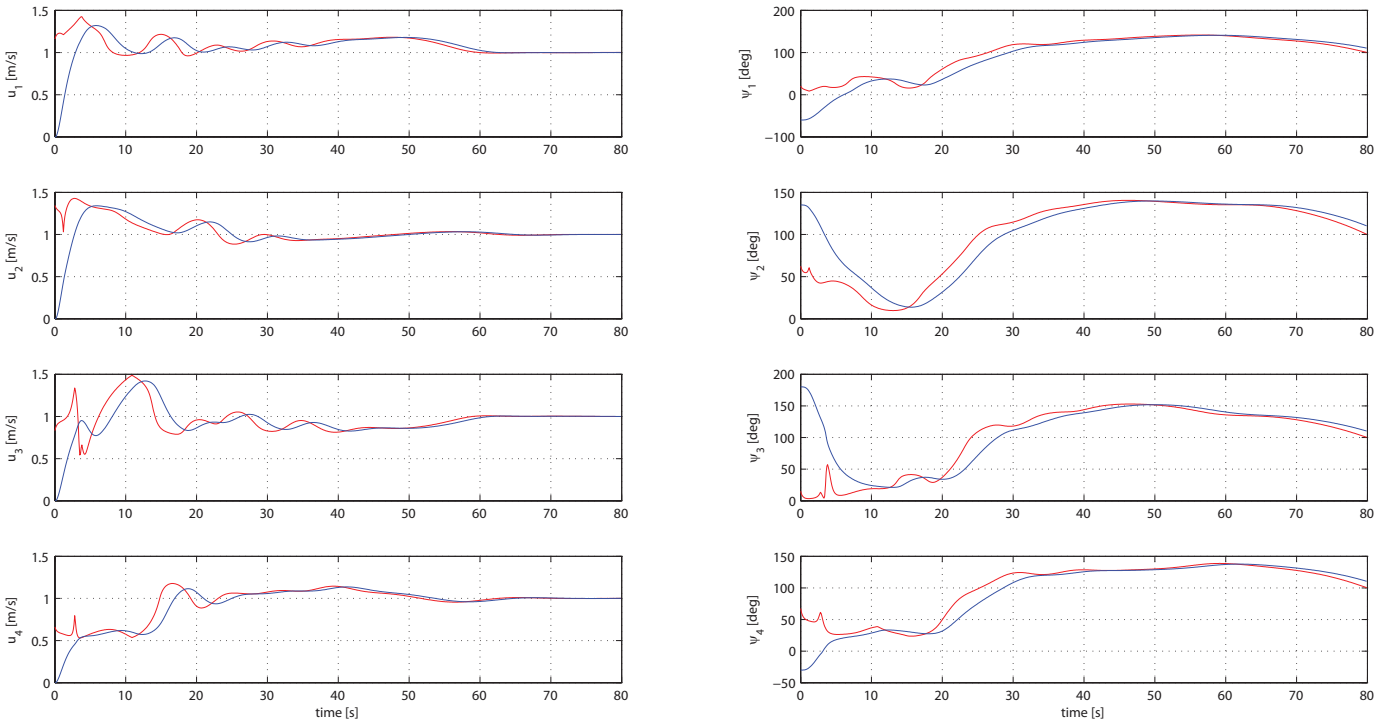

Fig. 8. Robots' speed and orientation profiles assumed during swarm aggregation combined with path-following guidance.

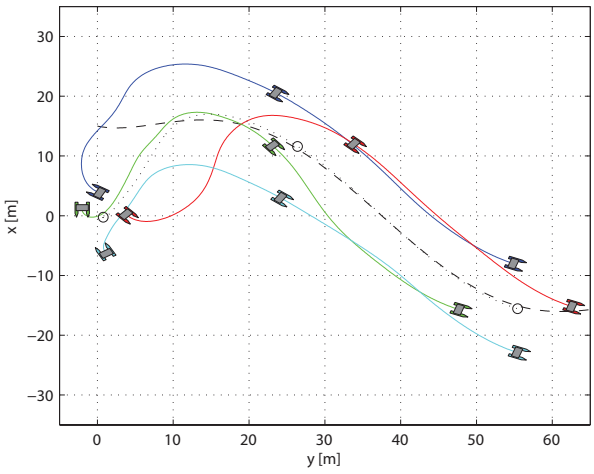

Fig. 7. Robots' motions during swarm aggregation combined with path-following guidance.

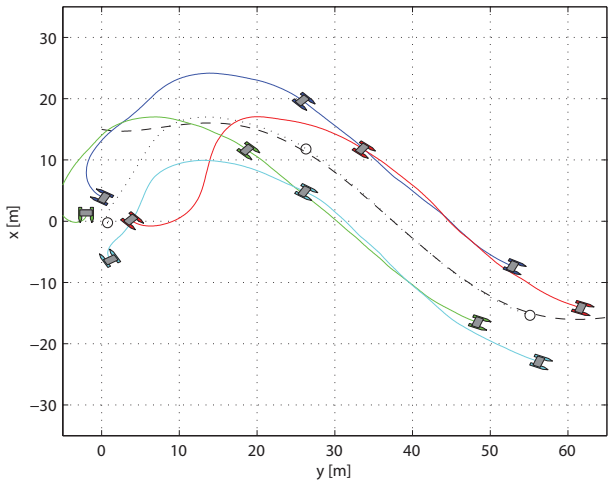

Fig. 9. Robots' motions during swarm aggregation combined with path-following guidance, with system affected by disturbance effects.

motion. The same experiment previously described is executed, adding two Gaussian noise signals to the orientation ψ_i and surge speed u_i of each vehicle. These disturbance signals represent the combined effects of model uncertainties, sensor noises and environmental disturbances affecting the framework. In particular, the two disturbance processes $N_u(\mu_u, \sigma_u)$ and $N_\psi(\mu_\psi, \sigma_\psi)$ are characterized by a zero mean value, $\mu_u = 0$ and $\mu_\psi = 0$, and standard deviations equal to $\sigma_u = 0.05$ and $\sigma_\psi = 0.01$. Figure 9 reports the motion of the vehicles and Figure 10 reports the speed and heading profiles, noticing that the generated signals are clearly affected by the disturbance, but the convergence to the required references is still guaranteed.

To stress the robustness of the proposed approach, an explicit disturbance signal representing a North-directed sea current of 0.25 m/s has been injected, in addition to the already present general disturbance of the previous experiment, to the vehicles' kinematic model. Figure 11 shows the variation of the motion evolution with respect to the previous experiment. In particular it is possible to notice the virtual motion of the formation centroid, affected by a reducing tracking error along the path. The zeroing of such an error relies on the capabilities of the dynamics' controller of rejecting static errors. Thus different regulator schemes, at dynamical level, can be introduced to overcome this issue. The speed and orientation behavior for

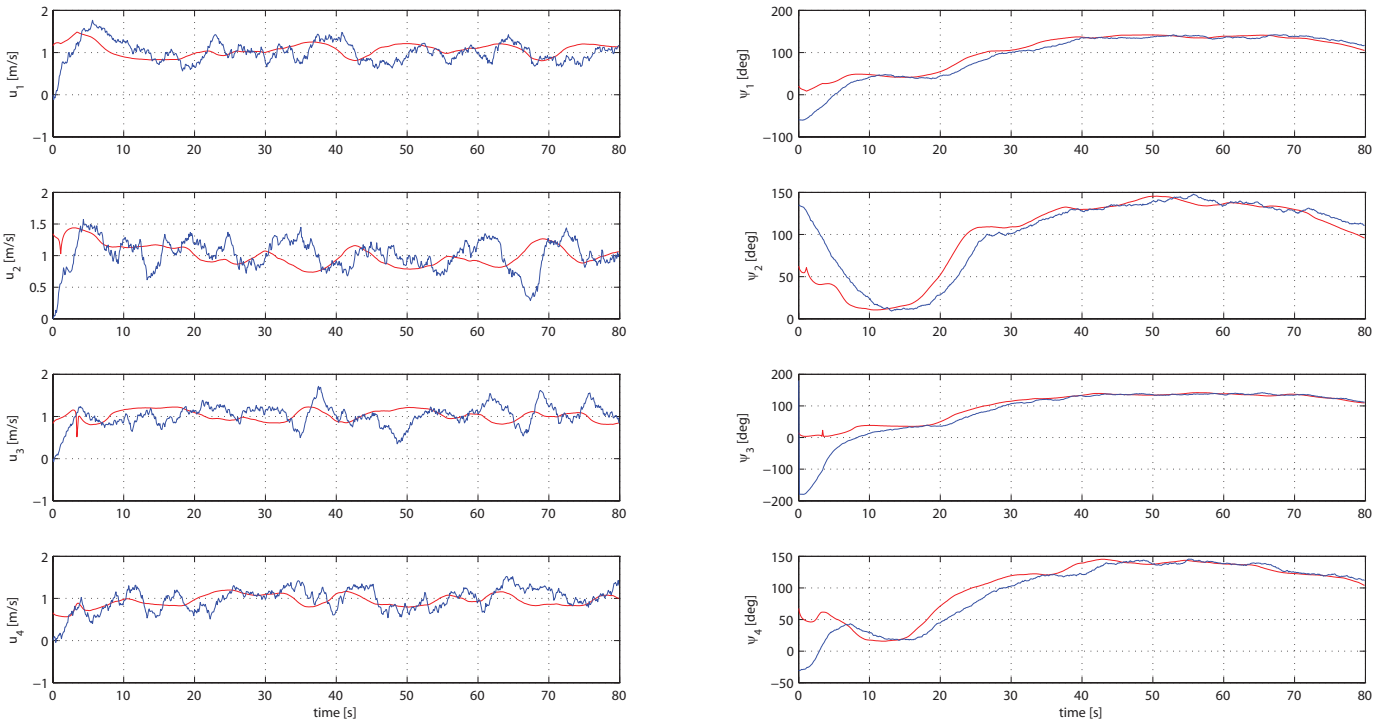

Fig. 10. Robots' speed and orientation profiles assumed during swarm aggregation combined with path-following guidance, with system affected by disturbance effects.

this experiment are reported in Figure 12.

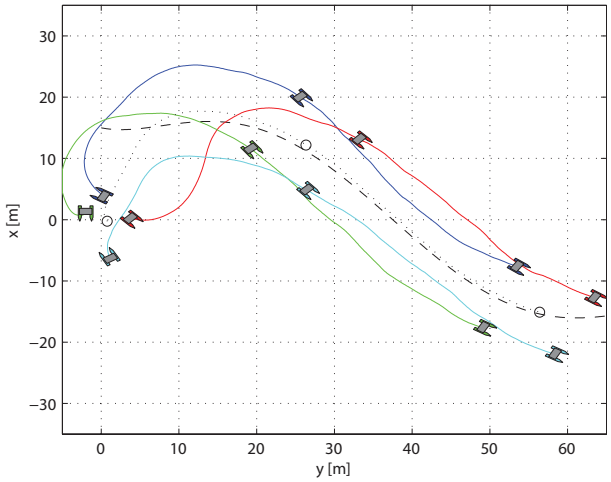

Fig. 11. Robots' motions during swarm aggregation combined with path-following guidance, with system affected by disturbances and sea current.

In order to highlight and practically validating the convergence of the combined approach from any initial configuration, already guaranteed by the theoretical analysis, two further experimental results are reported, again affecting the simulation execution with disturbance effects and constant sea current as the previous simulations. The motion of the robots starting from a parallel initial positioning is reported in Figure 13. The evolution of robots' motion from an aligned initial position configuration is shown in Figure 14.

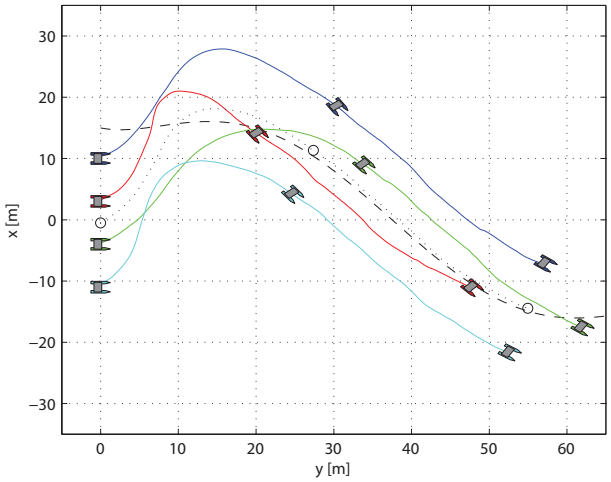

Fig. 13. Robots' motions starting from a parallel initial positioning.

A. *Remarks on the collision avoidance issue*

Unmanned Surface Vehicles are usually employed for exploration, observation and sampling tasks; to achieve satisfactory results during the execution of such tasks, "good" operating conditions are needed. The term "good" basically refers to environmental conditions characterized by moderate wind, sea currents and waves, in such a way that the motion of the vehicles is only marginally affected by the external disturbances. Anyway, being the proposed collision avoidance solution not formally proved, a statistical analysis based on a Monte Carlo simulation set has been carried out in order to analyze the practical collision avoidance implementation and evaluate the

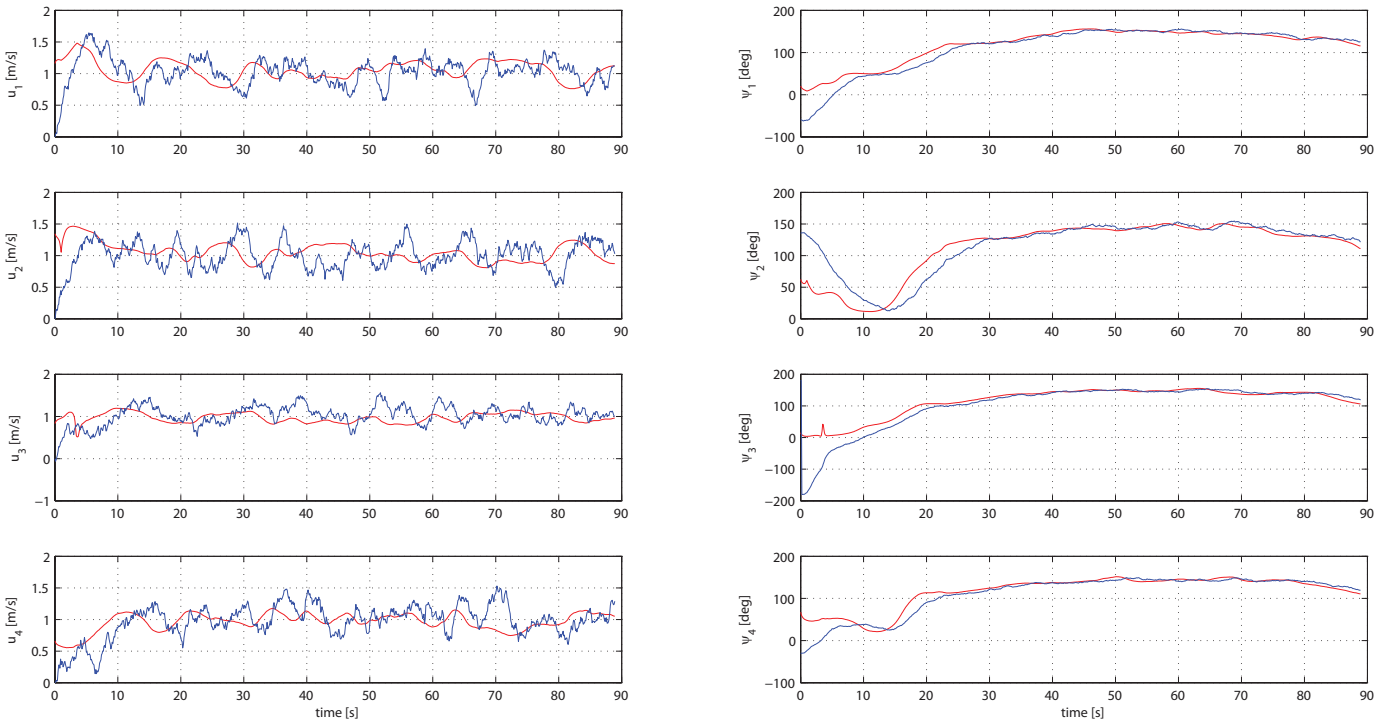

Fig. 12. Robots' speed and orientation profiles assumed during swarm aggregation combined with path-following guidance, with system affected by disturbances and sea current.

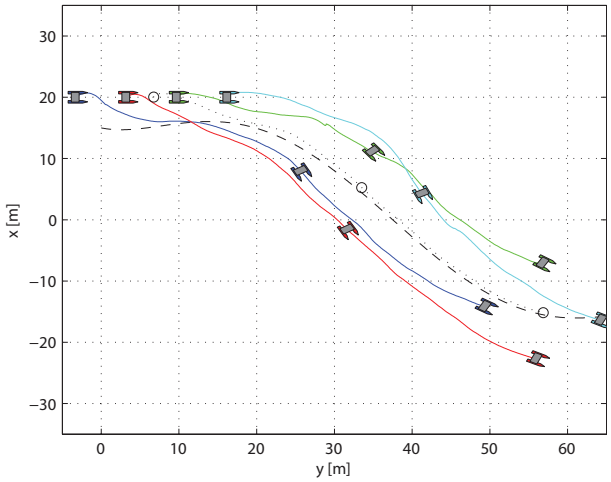

Fig. 14. Robots' motions starting from an aligned initial positioning.

functional limits of the adopted solution. With the aim of obtaining an overall indicator of the system performance with respect to the collision avoidance capability, the simulations are focused on the detection of the number of inter-vehicles collisions, when the motion of the vehicles is affected by an external disturbance, i.e., sea conditions.

Each simulation is executed requiring the robots' team to track the same sinusoidal path (already defined for the previous tests), affecting the robots' positions with two separate disturbance signal: a first one, constant during the entire simulation, representing a sea current; the second one, a randomly generated position error varying during the simulation, representing random wave and wind effects. At the beginning of each simulation a sea current setting is selected, randomly choosing a direction in $\left[0; \frac{\pi}{2}\right]$ and the current intensity characterized by a Gaussian distribution $N_d(0, \sigma_d)$. During the simulation the vehicles' positions are perturbed by a random disturbance characterized by the same Gaussian distribution $N_d(0, \sigma_D)$. During each simulation run, the number of collision is counted, where a collision is intended when the condition $d - 2\eta \leq 0$ is satisfied.

A number of 5 simulations sets have been executed, for each set a different σ_d is selected, i.e. increasing more and more the disturbance effect. For each set, a number of 1000 simulations is executed, collecting for each one the number of collisions and then producing, at the end of the simulations set, the statistics of average collision number μ_c and standard deviation σ_c.

The results of the simulations are reported in Table I.

It has to be remarked that the disturbance effects considered in simulation number 2 already represent limit operating conditions for vehicles' exploitation. As shown in the table, such a condition does not (statistically) influence the func-

TABLE I
COLLISION AVOIDANCE STATISTICS

Set #	σ_d	Simulations	μ_c	σ_c
1	0.025	1000	0	0
2	0.08	1000	0	0
3	0.14	1000	0.1370	0.6298
4	0.2	1000	2.5990	2.9204
5	0.25	1000	8.8600	6.0326

tionality of the adopted collision avoidance scheme. Thus the practical collision avoidance is proved under reasonable operating constraints.

X. Conclusions

In this paper, the integration of a swarm aggregation technique with a virtual target based path-following guidance controller has been reported. The easiness of the integration itself, given by the high modularity of both the swarm aggregation and path-following algorithms, as well as the theoretically proven feasibility of the techniques' integration, make the proposed approach appealing for practical application at sea. A set of test results has demonstrated the validity of the combined swarm-aggregation / path-following approach, also highlighting the robustness with respect to system disturbances and environmental effects (such as sea currents).

Future works are focused on the integration of connectivity information within the Swarm / Path-Following framework, with the aim of providing the capability of preventing the communication graph disconnection, i.e. allowing the vehicles to overcome the problems of connection blackouts or link changes, as it happens in dynamic networks. In particular, the aim is to extend the proposed approach to a general multi-vehicle marine framework, where heterogeneous agents (i.e. surface and underwater vehicles) can cooperate, keeping into account the strict constraint given by underwater communications provided by the acoustic links that are characterized by low bandwidth and reliability.

References

[1] A. Aguiar, J. Almeida, M. Bayat, B. Cardeira, R. Cunha, A. Hausler, P. Maurya, A. Oliveira, A. Pascoal, A. Pereira, M. Rufino, L-Sebastião, C. Silvestre, and F. Vanni. Cooperative autonomous marine vehicle motion control in the scope of the eu grex project: Theory and practice. In *OCEANS 2009-EUROPE*, pages 1–10. IEEE, 2009.

[2] Gerard Beni and Ping Liang. Pattern reconfiguration in swarms-convergence of a distributed asynchronous and bounded iterative algorithm. *Robotics and Automation, IEEE Transactions on*, 12(3):485–490, 1996.

[3] M.R. Benjamin, J.A. Curcio, J.J. Leonard, and P.M. Newman. Navigation of Unmanned Marine Vehicles in accordance with the rules of the road. In *Proc. of the IEEE International Conference on Robotics and Automation*, Orlando (FL), USA, May 2006.

[4] M. Bibuli, G. Bruzzone, M. Caccia, and L. Lapierre. Path-following algorithms and experiments for an unmanned surface vehicle. *Journal of Field Robotics*, 26(8):669–688, 2009.

[5] M. Bibuli, G. Bruzzone, M. Caccia, and L. Lapierre. Towards cooperative control of unmanned surface vehicles: experiments in vehicle-following. *IEEE Robotics & Automation Magazine*, 19(3):92–102, 2012.

[6] Liu Bo and Yu Hai. Flocking in multi-agent systems with a bounded control input. In *International Workshop on Chaos-Fractals Theories and Applications*, pages 130 –134, nov. 2009.

[7] M. Breivik. Formation control with Unmanned Surface Vehicles. Technical report, Centre for Ships and Ocean Structures; Norwegian University of Science and Technology, 2009.

[8] M. Breivik. *Topics in guided motion control of marine vehicles*. PhD thesis, Department of Engineering Cybernetics, Norwegian University of Science and Technology, 2010.

[9] M. Caccia, M. Bibuli, R. Bono, and G. Bruzzone. Basic navigation, guidance and control of an Unmanned Surface Vehicle. *Autonomous Robots*, 25(4):349–365, 2008.

[10] M. Caccia, M. Bibuli, R. Bono, Ga. Bruzzone, Gi. Bruzzone, and E. Spirandelli. Unmanned Surface Vehicle for coastal and protected water applications: the Charlie project. *Marine Technology Socety Journal*, 41(2):62–71, 2007.

[11] T. Chu, L. Wang, and T. Chen. Self-organized motion in anisotropic swarms. *Journal of Control Theory and Applications*, 1:77–81, 2003.

[12] T. B. Curtin, J. G. Bellingham, J. Catipovic, and D. Webb. Autonomous oceanographic sampling networks. *Oceanography*, 6(3):86–94, 1993.

[13] D.V. Dimarogonas and K.J. Kyriakopoulos. Connectedness preserving distributed swarm aggregation for multiple kinematic robots. *IEEE Transactions on Robotics*, 24(5):1213 –1223, oct. 2008.

[14] DV Dimarogonas, MM Zavlanos, SG Loizou, and KJ Kyriakopoulos. Decentralized motion control of multiple holonomic agents under input constraints. In *IEEE Conference on Decision and Control*, volume 4, pages 3390–3395, 2003.

[15] Joel M Esposito. Distributed grasp synthesis for swarm manipulation with applications to autonomous tugboats. In *IEEE International Conference on Robotics and Automation*, pages 1489–1494, 2008.

[16] E. Fiorelli, N. E. Leonard, P. Bhatta, D. A. Paley, R. Bachmayer, and D. M. Fratantoni. Multi-auv control and adaptive sampling in monterey bay. *IEEE Journal of Oceanic Engineering*, 31(4), 2006.

[17] Mauro Franceschelli and Andrea Gasparri. On agreement problems with gossip algorithms in absence of common reference frames. In *ICRA*, pages 4481–4486, 2010.

[18] C.L. Frey, D. Zarzhitsky, W.M. Spears, D.F. Spears, C. Karlsson, B. Ramos, J.C Hamann, and E.A. Widder. A physicomimetics control framework for swarms of autonomous surface vehicles. In *OCEANS 2008*, pages 1–6. IEEE, 2008.

[19] D. Fritsch, K. Wegener, and R.D. Schraft. Control of a robotic swarm for the elimination of marine oil pollutions. In *Swarm Intelligence Symposium, 2007. SIS 2007. IEEE*, pages 29–36. IEEE, 2007.

[20] A. Gasparri, G. Oriolo, A. Priolo, and G. Ulivi. A swarm aggregation algorithm based on local interaction for multi-robot systems with actuator saturations. In *2012 IEEE/RSJ International Conference on Intelligent Robots and Systems (IROS),*, pages 539 –544, oct. 2012.

[21] A. Gasparri, A. Priolo, and G. Ulivi. A swarm aggregation algorithm for multi-robot systems based on local interaction. In *2012 IEEE International Conference on Control Applications (CCA),*, pages 1497 –1502, oct. 2012.

[22] V. Gazi and K. M. Passino. A class of attractions/repulsion functions for stable swarm aggregations. *International Journal of Control*, 77(18):1567–1579, 2004.

[23] V. Gazi and K.M. Passino. Stability analysis of swarms. *IEEE Transactions on Automatic Control,*, 48(4):692 – 697, april 2003.

[24] F. Higgins, A. Tomlinson, and K.M. Martin. Survey on security challenges for swarm robotics. In *Fifth International Conference on Autonomic and Autonomous Systems, 2009. ICAS '09.*, pages 307 –312, april 2009.

[25] C. Karlsson, C.L. Frey, D.V. Zarzhitsky, D.F. Spears, and E.A. Widder. Physicomimetics for distributed control of mobile aquatic sensor networks in bioluminescent environments. In *Physicomimetics*, pages 145–191. Springer, 2012.

[26] H.K. Khalil. *Nonlinear Systems*. Prentice-Hall, New Jersey, second edition, 1996.

[27] D. Kostic, S. Adinandra, J. Caarls, N. van de Wouw, and H. Nijmeijer. Saturated control of time-varying formations and trajectory tracking for unicycle multi-agent systems. In *IEEE Conference on Decision and Control*, pages 4054 –4059, dec. 2010.

[28] J.R.T. Lawton, R.W. Beard, and B.J. Young. A decentralized approach to formation maneuvers. *IEEE Transactions on Robotics and Automation,*, 19(6):933 – 941, dec. 2003.

[29] A. Leccese, A. Gasparri, G. Oriolo, A. Priolo, and G. Ulivi. A swarm aggregation algorithm based on local interaction with actuator saturations and integrated obstacle avoidance. In *2013 IEEE International Conference on Robotics and Automation (ICRA 2013),*, pages 539 –544, oct. 2012.

[30] W. Li and X. Wang. Adaptive velocity strategy for swarm aggregation. *Physical Review Letters E*, 75, Feb 2007.

[31] Wei Li. Stability analysis of swarms with general topology. *IEEE Transactions on Systems, Man, and Cybernetics, Part B: Cybernetics*, 38(4):1084 –1097, aug. 2008.

[32] E. J. Lobaton, J. Zhang, S. Patil, and R. Alterovitz. Planning curvature-constrained paths to multiple goals using circle sampling. In *IEEE International Conference on Robotics and Automation*, pages 1463–1469, 2011.

[33] N. Miskovic, Z. Vukic, M. Bibuli, G. Bruzzone, and M. Caccia. Fast in-field identification of unmanned marine vehicles. *Journal of Field Robotics*, 8(1):101–120, 2011.

[34] R. Olfati-Saber and R. M. Murray. Consensus problems in networks of agents with switching topology and time-delays. *IEEE Transactions on Automatic Control*, 49(9):1520–1533, 2004.

[35] John H Reif and Hongyan Wang. Social potential fields: A distributed behavioral control for autonomous robots. *Robotics and Autonomous Systems*, 27(3):171–194, 1999.

[36] Craig W Reynolds. Flocks, herds and schools: A distributed behavioral model. In *ACM SIGGRAPH Computer Graphics*, volume 21, pages 25–34. ACM, 1987.

[37] L. Sabattini, C. Secchi, N. Chopra, and A. Gasparri. Distributed control of multirobot systems with global connectivity maintenance. *IEEE Transactions on Robotics*, 5(29):1326 – 1332, 2013.

[38] M. Schneider, T. Glotzbach, T. Güther, and P. Otto. Towards cooperative behaviour between multiple unmanned marine vehicles (mumvs): Team handling for the first multi vehicle primitives. In *Proceedings of the 8th International Conference on Computer Applications and Information Technology in the Maritime Industries COMPIT09*, pages 165–184, 2009.

[39] Y.K. Sharma and A. Bagla. Security challenges for swarm robotics. *SECURITY CHALLENGES*, 2(1):45–48, 2009.

[40] M. Varga, Z. Piskovic, and S. Bogdan. Multi-agent swarm based localization of hazardous events. In *Control and Automation (ICCA), 2010 8th IEEE International Conference on*, pages 1864–1869. IEEE, 2010.

[41] Peng Yang, Randy A Freeman, Geoffrey J Gordon, Kevin M Lynch, Siddhartha S Srinivasa, and Rahul Sukthankar. Decentralized estimation and control of graph connectivity for mobile sensor networks. *Automatica*, 46(2):390–396, 2010.